Influence of Diffuser on Aerodynamic Noise of a Forward Curved Fan

Soichi SASAKI*, Kota SUZUKI, Yuta Onomichi** and Hidechito Hayashi***

* Division of System Science, Graduate School of Engineering, Nagasaki University, 1-14 Bunkyo-machi Nagasaki 852-8521, Japan
** Department of Advanced Engineering, Graduate School of Engineering, Nagasaki University, 1-14 Bunkyo-machi Nagasaki 852-8521, Japan

In order to clarify the influence of a diffuser on the characteristics of a forward curved fan, the influence of the bare ratio and the outlet angle on the characteristics of the fan were measured through an experiment performed with an actual fan as well as through a numerical simulation, respectively. The mechanism of the discrete frequency noise generated by the separated flow of the diffuser was analyzed. The optimized bare ratio was approximately 17°. The flow separated inside of the diffuser generated discrete frequency noise owing to the interaction between the reversed flow from the diffuser and the impeller rotating at the blade passing frequency. The diffuser made by the outlet angle increased the pressure ratio more than that made by the bare ratio. Furthermore, it was confirmed that restraining the separation in the diffuser effectively decreases the fan noise.

Keywords: Pressure Drop, Fan, Aerodynamic Noise, Internal Flow, Separation

CLC number: **Document code: A** **Article ID:**

Introduction

Forward curved fans are used in everyday environments. Because these appliances are often continuously driven for long periods, high aerodynamic efficiency is essential to limit energy consumption. Moreover, it is necessary for not only maximized fan efficiency, but also minimized fan noise in order to ensure a comfortable living environment. When the clearance for the tongue of the diffuser is optimized, the discrete frequency noise of the fan can be restrained to the broadband noise level [1]. In a previous study, the discrete frequency noise of the centrifugal fan was recognized as the noise caused by the interaction between the wake of the impeller and the tongue [2]. Optimizing the diffuser also improves the aerodynamic characteristics and decreases the fan noise. Kodama et al. experimentally clarified the influence of the scroll angle on both the aerodynamic characteristics and the noise of a dual-cascade centrifugal fan [3]. However, there have been few practical studies that focus on the relationship between the design conditions of the diffuser and the internal flow; the studies discussing the aerodynamic noise depended on the design parameters of the diffuser are also rare. In particular, information regarding the influence of the bare ratio on the fan noise is hardly found except for the experiment that Hatakeyama et al. reported on the noise analysis of the dual-cascade centrifugal fan [4].

In this study, in order to clarify the mechanism by which the diffuser affects the aerodynamic noise of the fan, the influence of the bare ratio and the outlet angle on the fan characteristics was analyzed. Based on the analysis of the aerodynamic noise source and the internal flow from a computational fluid dynamics (CFD), the mechanism of the fan noise that is affected by the design conditions of the diffuser is discussed.

Fig. 1 Test impeller

Table 1 Dimensions of the impeller

Diameter , D (mm)	125
Chord Length , C (mm)	9
Number of Blades , Z	40
Span Length , b (mm)	50
Shroud	front shroud / rear shroud

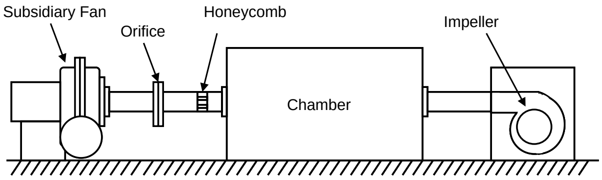

Fig. 2 Method for measuring the aerodynamic characteristics

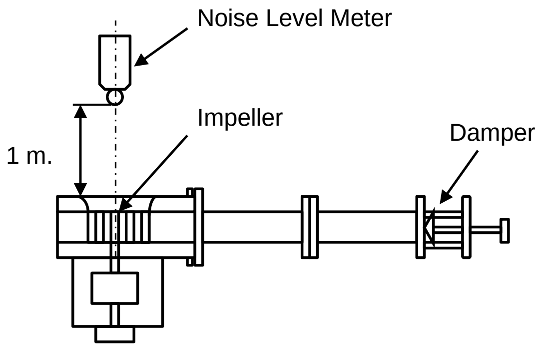

Fig. 3 Method of measuring the fan noise

Experimental Procedure

The test impellers are shown in Fig. 1. The main dimensions are listed in Table 1. A two-dimensional forward curved blade was employed for the impeller. Fig. 2 shows the schematic view of the experimental apparatus for estimating the aerodynamic characteristics. The static pressure was measured in the plenum chamber, which has dimensions of □500 mm × 900 mm. The

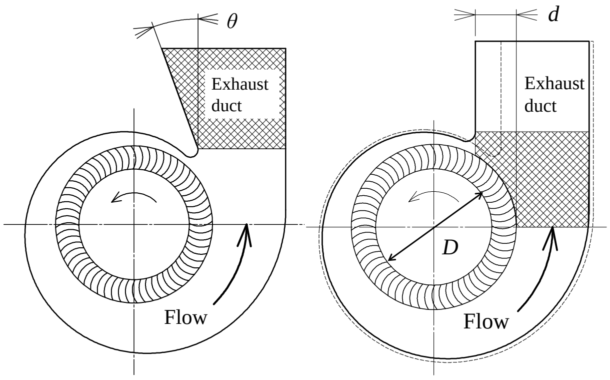

(a) Outlet angle (b) Bare ratio

Fig. 4 Diffuser in the scroll casing with respect to two different parameters

Table 2 Summary of the diffuser conditions in the experimental apparatus

No.	α , °	e , %	θ , °
1	6.0°	9%	0°
2	6.0°	25%	0°
3	6.0°	25%	20°

normalized aerodynamic characteristics of the fan are defined as Eq. (1).

$$\psi = \frac{2P_s}{\rho U^2}, \phi = \frac{Q}{60\,\pi\, D\, b\, U}$$
$$\lambda = \frac{2L}{\rho\,\pi\, D\, b\, U^3}, \eta = \frac{\varphi\,\psi}{\lambda} \quad (1)$$

where ψ is the static pressure coefficient, φ is the flow coefficient, λ is the power coefficient, and η is the efficiency. The rotational speed was set to 2800 rpm. The method for measuring the fan noise is shown in Fig. 3. The noise was measured using a noise level meter (ONO SOKKI, LA4350) at an observation point that was 1.0 m above the bell mouth and situated along the axis of the motor. The noise data were input to FFT analyzer (ONO SOKKI, CF5210) to evaluate the noise spectrum. The diffuser in the scroll casing is presented in Fig. 4. The parallel wall diffuser has a scroll angle of 6°. The θ in the Fig. 4(a) represents the outlet angle. The diffuser is formed in the exhaust duct of the scroll casing when the scroll angle θ is given. The bare ratio of the diffuser is depicted schematically in Fig. 4(b). The bare ratio is defined as the ratio of the diameter of the impeller to the

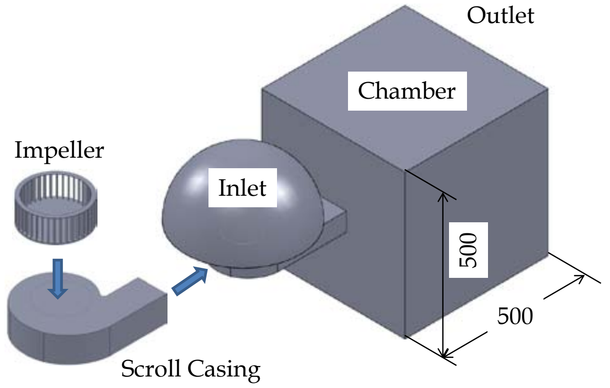

Fig. 5 Model for the numerical simulation

Table 3 Summary of the design conditions of the diffuser in the numerical simulation and the experiment

Outlet Angle , θ (°)	0	5	10	15	20	25	30			
Bare Ratio (%)	9									
EFD	○				○					
CFD	○	○	○	○	○	○	○			

Bare Ratio (%)	0	2.5	5	9	13	17	20	25	30	40
Outlet Angle , θ (°)	0									
EFD				○				○		
CFD	○	○	○	○	○	○	○	○	○	○

bare length ($e = d / D$). The diffuser is represented by the shaded region in the figure. In the experiment with an actual fan, the relationship between the diffuser conditions listed in Table 2 and the resulting characteristics was estimated.

The three-dimensional model of the fan for the CFD is shown in Fig. 5. The representative length of the impeller and the diffuser is modeled equivalently to the actual system. The □500 mm × 500 mm chamber was attached to the outlet of the diffuser. Table 3 lists the design parameters of the scroll casing for estimating the fan characteristics in the numerical simulation. For evaluating the resulting characteristics with respect to the outlet angle, models from 0° to 30° were created. For estimating the resulting characteristics with respect to the bare ratio, ten models with values between 0% and 40% were created. The CFD code of SCRYU/Tetra produced by Software Cradle Co., Ltd. was used for the numerical simulations. Approximately 6.5 million grid elements were employed to solve the entire steady flow field of the fan. The SST *k-ω* model was employed to simulate the turbulent model. A constant flow rate was set at the inlet boundary of the model; the atmospheric pressure (0 Pa) was set at the outlet side.

Powell [5] studied the theoretical sound sources in a flow field, and Howe [6] mathematically presented the sound source as Eq. (2).

$$\frac{\partial^2 p_a}{\partial t^2} - c^2 \nabla^2 p_a = \rho_0 div(\vec{\omega} \times \vec{u}) \tag{2}$$

where $\vec{\omega}$ is the vorticity vector and $\vec{u}$ is the velocity vector. The spatial distribution of the sound source can be visualized by using the right-hand side of Eq. (2).

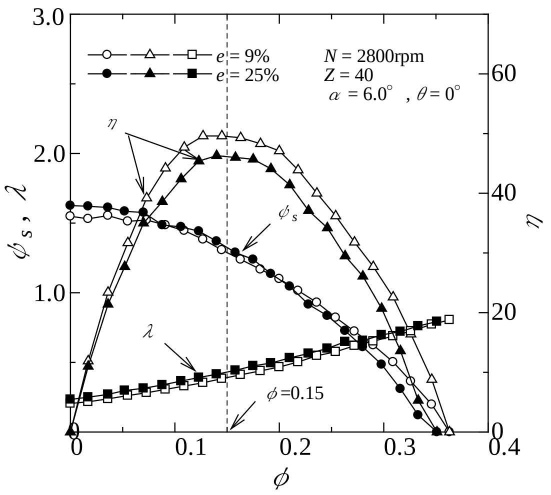

Fig. 6 Comparison of the aerodynamic characteristics for different bare ratios

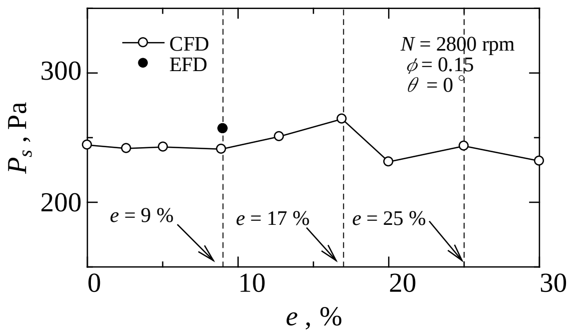

Fig. 7 Static pressure with respect to the bare ratio

Results and Discussion

The aerodynamic characteristics of the fan for different bare ratios are compared in Fig. 6. The maximum efficiency point of the fan is in the vicinity of φ = 0.15. At the maximum efficiency point, the static pressure coefficient is approximately equivalent; however, the fan efficiency for e = 9% is 3.3% higher

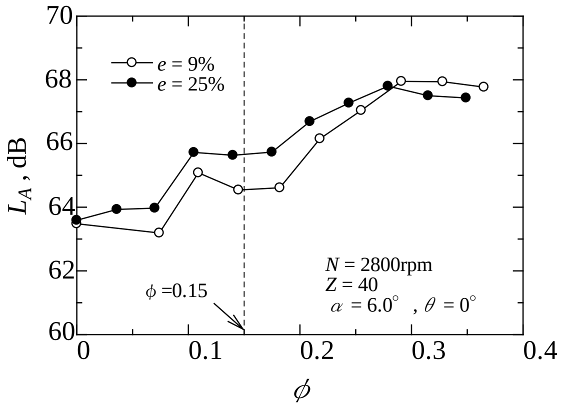

Fig. 8 Comparison of the fan noise for different bare ratios

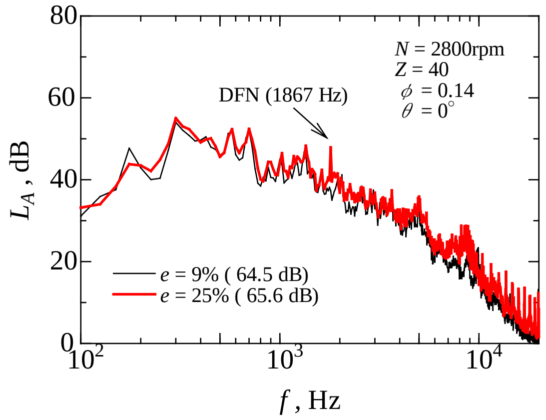

Fig. 9 Spectral distribution of the fan noise for different bare ratios

than that for e = 25%. The relationship between the bare ratio and the static pressure coefficient is shown in Fig. 7. The error of the measured static pressure coefficient at e = 9% and the calculated value was 6.9%. When the bare ratio increases from 9% to 17%, the static pressure coefficient increases 9.7%, whereas if the bare ratio surpasses 17%, the static pressure rapidly decreases. The noise characteristics of the fan are shown in Fig. 8. In the vicinity of the maximum efficiency, the fan noise at e = 25% is approximately 1 dB larger than that for e = 9%. In Fig. 9, the two noise spectra for different bare ratios are compared. The thick (red) line represents the noise level at e = 25%, and the thin (black) line represents that at e = 9%. The blade passing frequency (BPF) is 1867 Hz. Both broadband noise levels are approximately equivalent, but the discrete frequency noise at the BPF for e = 25% is larger than that for e = 9 %. This is a reason the fan noise of e = 25% is larger than that of e = 9%.

The sound sources and velocity vectors of the fan modeled by CFD are shown in Fig. 10. For the case e = 9%, a vortex due to recirculation flow is formed at point A. For the case of diffuser made by a low bare ratio (point B), a dead air region due to the stagnation flow was formed. When the flow impinges the wall of the duct, a secondary flow that travelled up and down was formed (C point). For the case of e = 17%, a vortex pair with

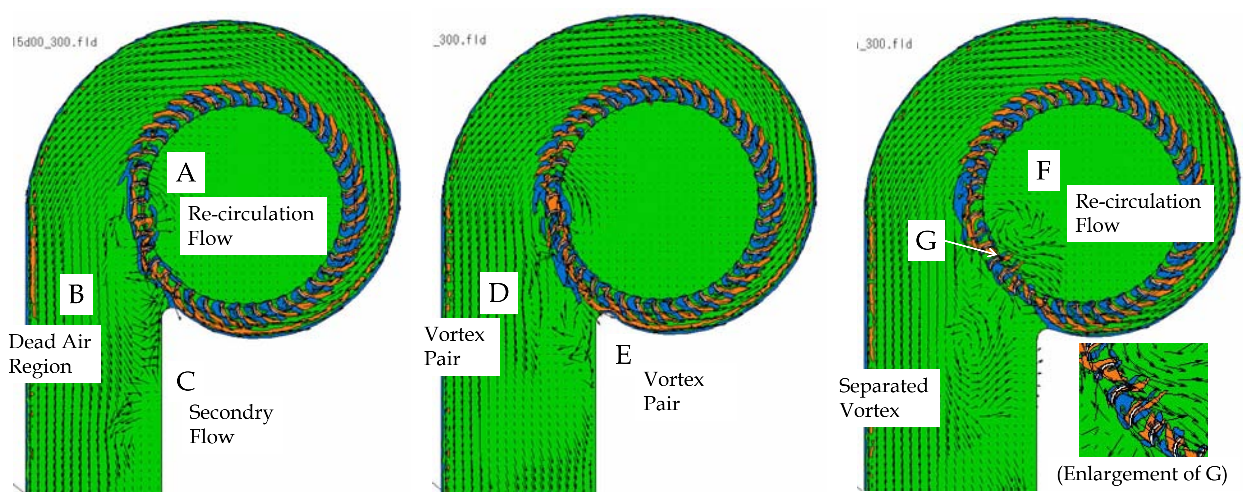

(a) e = 9% (b) e = 17% (c) e = 25%

Fig. 10 Distribution of the aerodynamic noise sources and the velocity vectors for different base ratios

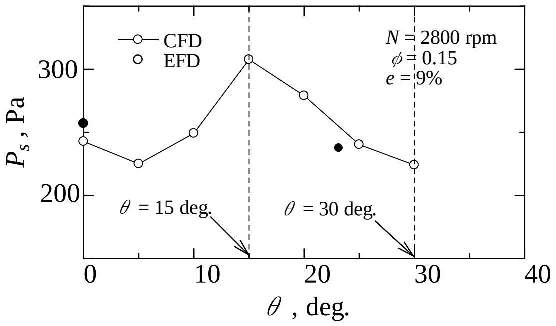

Fig. 11 Static pressure with respect to the outlet angle

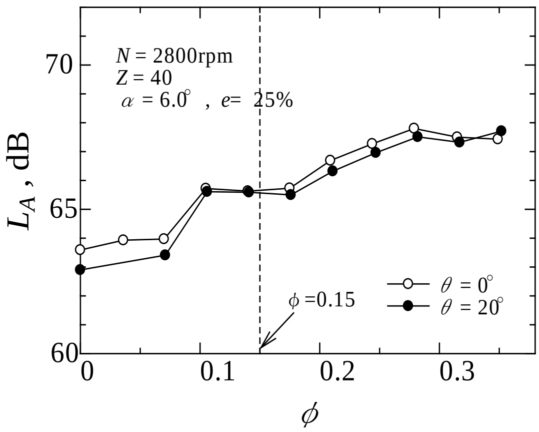

Fig. 12 Comparison of the fan noise characteristics for different outlet angles

different rotations was formed (points D and E). Mainly, the deformation of the shear layer in the main flow domain was eased according to the rotation of the vortex at point E. For the case of e = 25%, the vortex due to the recirculation flow was formed at point F in the figure. In this case, the large vortex flow was formed by the diffusion. At the point of interaction between the separated flow and the recirculation flow (point G), a backward flow towards the inside of the impeller occurred. For the distribution of the sound source, only the case of e = 25% formed a strong aerodynamic sound source. From the fan with e = 25%, it was clarified that the discrete frequency noise was generated because of the interaction between the backward flow and the rotating impeller at the BPF (see Fig. 9).

The relationship between the outlet angle and the static pressure obtained from the numerical simulation is shown in Fig. 11, in which the bare ratio of the model is 9%. For the case of 0°, the error between the measured static pressure and the CFD is 5%. When the outlet angle increases from θ = 5° to θ = 20°, the static pressure increases by 36.8%. The outlet angle has a larger effect on the pressure rise of the diffuser than the bare ratio. When the outlet angle surpasses 15° the static pressure decreases because of the influence of separation. The

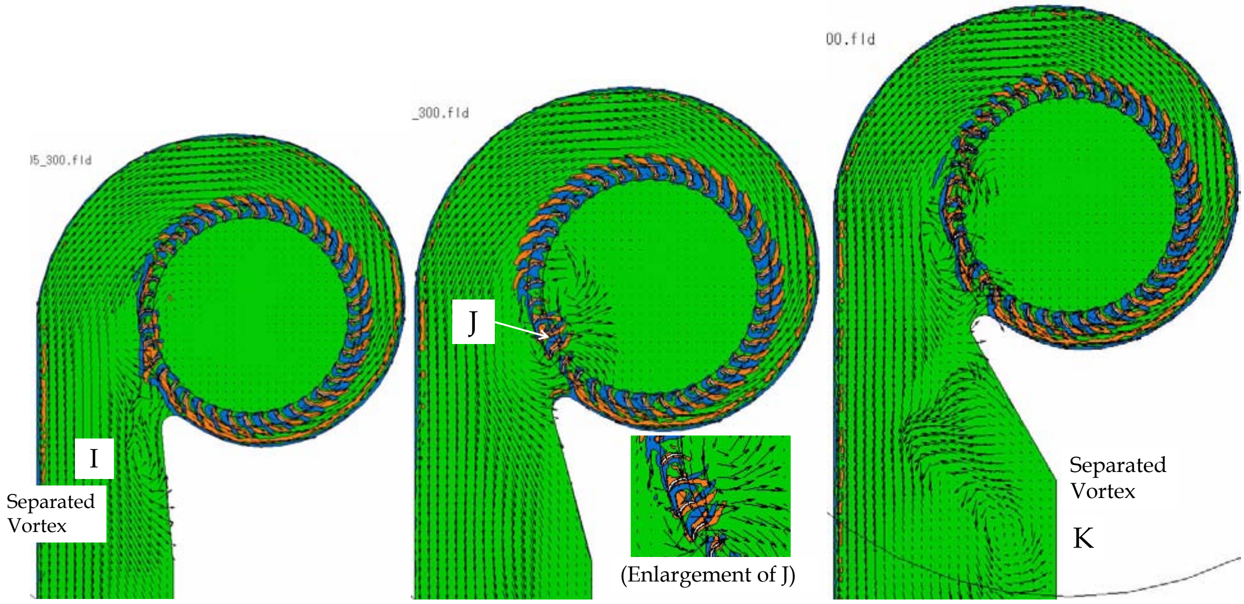

(a) θ = 5°　　(b) θ = 15°　　(c) θ = 30°

Fig. 13 Distribution of the aerodynamic noise sources and the velocity vectors for different outlet angles characteristics of the measured fan noise for two outlet angles are compared in Fig. 12, in which the bare ratio is 25%. The difference of the fan noise is less than 0.5 dB for the wide flow rate domain.

The aerodynamic sound sources and the velocity vectors of the fan are superimposed in Fig. 13. For the case of the outlet angle 5°, the separated vortex is formed at the diffuser (point I). This is an obstacle for the gentle deformation of the stream line. For the case of the angle 15°, the separated vortex is not formed at the diffuser. However, the flow that expanded in the diffuser interferes with the recirculation flow, forming the backward flow towards the inside of the impeller. In the vicinity of the backward flow, a strong aerodynamic noise source is generated (point J). In this case, the discrete frequency noise is generated because of the interaction between the backward flow and the impeller.

Conclusions

(1) The optimized bare ratio of the forward curved fan exists in the vicinity of 17%. Because the internal flow of the diffuser with a bare ratio larger than the optimized value separates, the static pressure of the forward curved fan did not rise.
(2) The separated flow inside the diffuser generated a discrete frequency noise because of the interaction between the backward flow from the diffuser and the impeller rotating at a BPF.
(3) The diffuser caused by the outlet angle contributed to the pressure rise of the fan than the diffuser by the bare ratio. Restraining the diffuser separation effectively decreases the fan noise.

References

[1] S. Sasaki, A. Kuroda and H. Hayashi.: A Study of Discrete Frequency Noise by Interaction between Wake of a Centrifugal Impeller and a Cylinder, Proceedings of the 10th International Symposium on Experimental Computational Aerothermodynamics of Internal Flows, Brussels, CD-ROM, (2011).
[2] Y. Ohta, E. Outa amd K. Tajima.: Evaluation and Prediction of Blade-Passing Frequency Noise Generated by a Centrifugal Blower, Journal of Turbo Machinery, Vol. 118, No. 3, pp.597–605, (1996).
[3] Y. Kodama, H. Hatakeyama, S. Sasaki and K. Goto: Study of Aerodynamic Characteristics and Noise of a Dual-cascade Centrifugal Fan (Effect of Scroll Angle and Partition), Turbomachinery (in Japanese), Vol. 29, No. 8, pp.456–463, (2001).
[4] M. Hatayeyama, Y. Kodama, S. Sasaki, H. Hayashi and K. Goto: Characteristics of the Aerodynamics and the Noise of a Dual-cascade Centrifugal Fan (Effects of Bare Ratio and Outlet Angle of Scroll Casing), Turbomachinery (in Japanese), Vol. 30, No. 2, pp.27–34, (2002).
[5] A. Powell: Theory of Vortex Sound, Journal of the Acoustic Society of America, Vol. 36, No. 1, pp. 177–195, (1964).
[6] M. S. Howe: Theory of Vortex Sound, Cambridge University Press, Cambridge, (2003).